Applied Catalysis A: General 513 (2016) 47–52

Contents lists available at ScienceDirect

Applied Catalysis A: General

journal homepage: www.elsevier.com/locate/apcata

A simple strategy towards the preparation of a highly active bifunctionalized catalyst for the deacetalization reaction

Shuai Chen [a], Fengwei Zhang [b,*], Mengqi Yang [c], Xincheng Li [c], Helong Liang [c], Yan Qiao [a,**], Dongyan Liu [a], Weibin Fan [a]

[a] Analytical Instrumentation Center, Institute of Coal Chemistry, Chinese Academy of Sciences, Taiyuan 030001, PR China
[b] Institute of Crystalline Materials, Shanxi University, Taiyuan 030006, PR China
[c] School of Chemistry and Chemical Engineering, Shanxi University, Taiyuan 030006, PR China

ARTICLE INFO

Article history:
Received 5 November 2015
Received in revised form
14 December 2015
Accepted 26 December 2015
Available online 30 December 2015

Keywords:
Bifunctional catalyst
Deacetalization reaction
Biphasic system
Pickering emulsion

ABSTRACT

A bifunctional catalyst containing both the hydrophobic methyl and hydrophilic sulfonic acid groups has been successfully fabricated by mild surface modification of the pre-prepared silica nanoparticles. To its credit, the methyl groups in the catalyst were applied to improve the surface wettability of silica solid nanoparticles, while the sulfonic acid groups were devoted to catalyzing the deacetalization of various acetal derivatives. The catalyst was characterized in detail by Scanning electron microscope (SEM), Transmission electron microscopy (TEM), Fourier-transform infrared spectroscopy (FT-IR) and Thermogravimetric analysis (TGA). The catalytic results revealed that the bifunctional SiO_2—Me&SO_3H NPs exhibited superior activity for the deacetalization of 4-methoxybenzaldehyde dimethyl acetal and the product conversion could be >99% within 45 min in the toluene/water biphasic system. The main reason was probably due to the formation of Pickering emulsion, which could greatly improve the interface area between the oil and water and decrease the mass transfer resistance

1. Introduction

Pickering emulsions (solid particles-stabilized emulsions) are colloidal emulsions that are stabilized by solid particles instead of traditional surfactant molecules [1,2]. In principle, the solid particles with appropriate hydrophilicity/hydrophobicity (wettability) can be strongly adsorbed at the interface between two immiscible fluids such as oil and water, creating an effective steric/electrostatic shield for the emulsified droplets [3–5]. And in terms of the wettability of the solid particles, the Pickering emulsion can be classified into either oil-in-water (O/W) or water-in-oil (W/O) type of emulsion. Generally, the hydrophilic particles tend to form O/W emulsion, while the hydrophobic particles prefer to generate W/O emulsion [6,7]. Beyond that, these solid particles-stabilized emulsions also offer unique advantages over traditional surfactant including reduced foaming, strong kinetic hindrance to droplet coalescence and tunable interfacial permeability. More recently, the researchers have demonstrated that the Pickering emulsions hold great promise in a variety of potential applications ranging from food production, cosmetics, coating and catalysis to petroleum industries [8–12].

Particularly, the intense research has been fueled by the development of Pickering emulsion catalyst for alcohol oxidation [13], alkene epoxidation [14], nitroarenes hydrogenation [15,16] and biofuel upgrade reactions [17–20]. Among them, the solid nanoparticles-stabilized emulsion catalytic system, in which the solid nanoparticles serve as both emulsifiers and catalysts, has proven superior to traditional surfactant-stabilized emulsion due to its easy separation and high recyclability [21,22]. To date, various solid particles including SiO_2 NPs, Fe_3O_4 NPs, TiO_2 NPs, zeolites, carbon nanotubes (CNTs) as well as their composites with appropriate wettability can be well located at the interface between the oil/water two phase [23–28]. Moreover, after immobilizing the catalytically active species onto the above support surface, they are likely to seat at the amphiphilic catalyst-stabilized Pickering emulsion droplet interface. In this regard, the resulting plentiful micro-size nanoreactors not only greatly increase the oil/water biphase contact area but also substantially reduce the transfer resistance of organic substrates and avoid the self-aggregation and leaching of catalytic active sites during the reaction [29].

The integration of amphiphilic solid nanomaterials and metal nanoparticles has been a fruitful area in hydrogenation [30], oxidation [31], biomass conversion [32] and esterification reactions

* Corresponding author.
** Corresponding author.
E-mail addresses: fwzhang@sxu.edu.cn (F. Zhang), qiaoy@sxicc.ac.cn (Y. Qiao).

http://dx.doi.org/10.1016/j.apcata.2015.12.036
0926-860X/

[33]. These studies proved that the solid catalyst materials with amphiphilic properties can not only significantly accelerate the reaction rate but also optimize the product selectivity to a certain extent. The possible reason was that they could greatly improve adsorption of substrates on the catalytic activity sites at the oil–water biphasic interfaces and exclude the product from the catalyst surface simultaneously. But as far as we know, the amphiphilic metal-free solid nanoparticles for the heterogeneous catalytic reaction in oil–water biphasic systems are still rarely reported [34]. In the current work, we present a simple strategy towards the preparation of a highly active metal-free bifunctionalized catalyst for the deacetalization reaction. The catalyst was prepared via the simultaneous modification of the silica nanoparticles surface with the hydrophobic methyl and hydrophilic sulfonic acid organosilanes. The deacetalization results demonstrated that the amphiphilic SiO_2—Me&SO_3H catalyst possessed excellent catalytic activity and stability in toluene/water biphasic system.

2. Experimental

2.1. Materials and methods

2-(4-Chlorosulfonylphenyl) ethyltrichlorosilane in methylene chloride (CSPETS) was purchased from J&K Co., Ltd. Methyltrichlorosilane (MTCS), tetraethyl orthosilicate (TEOS) and aqueous ammonia (25 wt%) were purchased from Aladdin Chemical Reagent Co., Ltd. All other chemicals and reagents were analytical grade and used without further purification. Deionized water was used in the whole experiment.

2.2. Preparation of the solid silica nanoparticles (SiO_2 NPs)

The SiO_2 NPs were synthesized by the classical Stöber method and with slight modification. Typically, 20 mL of aqueous ammonia (25 wt%) was added into the mixture of 400 mL of ethanol and 50 mL of deionized water via ultrasonication. After vigorously stirring for 30 min, 20 mL of TEOS was added slowly, and the mixture was stirred for another 6 h to obtain the uniform silica nanparticles. The resulting products were recovered through centrifugation and washed several times with deionized water and ethanol, and then dried at 50 °C under vacuum for 12 h.

2.3. Preparation of methyl and sulfonic acid bifunctionalized SiO_2 NPs (SiO_2—Me&SO_3NPs)

The synthesis of SiO_2—Me&SO_3H NPs was based on the co-condensation of 2-(4-chlorosulfonylphenyl) ethyltrichlorosilane (CSPETS) and methyltrichlorosilane (MTCS) in the presence of the silica nanoparticles, which was based on our previously reported work [35]. In a typical procedure, 1.0 g of SiO_2 NPs were dispersed into 50 mL of dry toluene via ultrasonication, then MTCS (0.4 mL, 3.0 mmol) and CSPETS (0.25 mL, 0.5 mmol) were slowly added into above mixture. The resulting mixture was stirred for 24 h at room temperature, and then it was washed three times with ethanol and each time was 15 mL. Subsequently, the solid samples were suspended in 1 M H_2SO_4 (50 mL) solution for 4 h, washed with a large amount of deionized water and dried at 50 °C under vacuum for 12 h to give the corresponding SiO_2—Me&SO_3H NPs. Elemental analysis result of the as-prepared catalyst revealed that the content of carbon, hydrogen and sulfur was 4.05 wt%, 1.69 wt% and 0.45 wt%, respectively.

2.4. Determination of the SiO_2—Me&SO_3catalyst***'s acidity***

The concentration of sulfonic acid groups was determined by ion-exchange pH analysis protocol [36]. Typically, 50 mg of SiO_2—Me&SO_3H catalyst was added to a 25 mL of 1.0 M NaCl aqueous solution, and the resulting suspension was stirred at room temperature for 48 h until equilibrium was reached. The filtrate was titrated with 50 mM NaOH and phenolphthalein was applied as indicator. The acid amount of SiO_2—Me&SO_3H catalyst was determined to be 0.14 mmol g^{-1}, which was highly consistent with the elemental analysis result.

2.5. General procedure for the hydrolysis reaction of acetal derivatives

The hydrolysis reaction of acetal derivatives was performed in a 10 mL of round bottom flask. A typical reaction process was as follows: 45 mg of SiO_2—Me&SO_3H NPs (6.3 μmol of —SO_3H groups) was put into the reactor, 3.0 mL of toluene and 3.0 mL of deionized water were added as solvent. After stirring for 5 min, 1 mmol of benzaldehyde dimethyl acetal was added into above mixture by syringe. The hydrolysis reaction was carried out at 30 °C for 45 min. After the reaction, the product was obtained through centrifugation and then the supernatant was determined by Agilent 7890A GC. Then the catalyst was recovered and washed several times with deionized water and ethyl acetate, dried at 50 °C for 2 h, and subsequently used in the next cycles.

3. Results and discussion

The morphology and structure of SiO_2 NPs and SiO_2—Me&SO_3H NPs were firstly elucidated by SEM. The representative SEM images of the as-prepared SiO_2 NPs and SiO_2—Me&SO_3H NPs are shown in Fig. 1a and b, the low magnification SEM image illustrated the large-scale formation of uniform monodisperse spherical SiO_2 NPs and SiO_2—Me&SO_3H NPs with an average diameter of ~150 nm. The TEM image (Fig. 1c and d) showed that the SiO_2—Me&SO_3H NPs have a rough surface compared with the pure SiO_2 NPs, indicating that each nanosphere consists of SiO_2 and —Me&SO_3H organic silane and the presence of —Me&SO_3H affected the morphology of SiO_2, which was consistent with the FT-IR results.

Fig. 2 shows the digital photographs and optical microscopy images of SiO_2—Me&SO_3H NPs-stabilized Pickering emulsions. The formation process of Pickering emulsions was as follows: 30 mg of SiO_2—Me&SO_3H NPs, 3 mL of toluene and 3 mL of water were added into a 10 mL of glass vial. The mixture was sonicated for 2 min and then violently stirring for another 5 min, and then standing for 1 h for optical microscope analysis. As can be seen in Fig. 2a, the whole materials were participated into the production of the emulsion and the height of the emulsion layer was about 0.95 cm, while the height of the upper toluene was approximately 0.44 cm. Thus, it can be speculated that the emulsification efficiency reached up to 68%. As for Fig. 2b, the optical microscopy image revealed that the SiO_2—Me&SO_3H NPs-stabilized Pickering emulsions with ellipsoidal shape and the droplets size were below 300 μm, which were well-dispersed on the glass slide. More importantly, the obtained emulsion could greatly improve the interface area between the oil and water and decreased the mass transfer resistance.

FT-IR spectroscopy was employed to verify the successful modification of —Me&SO_3H groups on the as-synthesized SiO_2 NPs. As shown in Fig. 3a, FT-IR spectra of the SiO_2 NPs around 1110 cm^{-1} and 795 cm^{-1} corresponded to the antisymmetric and symmetric stretching vibrations of Si—O—Si bond in oxygen–silica tetrahedral, respectively. The presence of the anchored alkyl groups was confirmed by the aliphatic weak C—H stretching vibrations appearing at 2975 cm^{-1} and 2884 cm^{-1} in the SiO_2—Me&SO_3H NPs. An increased intensity and broadening of the band at 3000–3500 cm^{-1} in the samples suggested the existence of more —OH groups on the SiO_2—Me&SO_3H NPs. Taken together, these results indicated

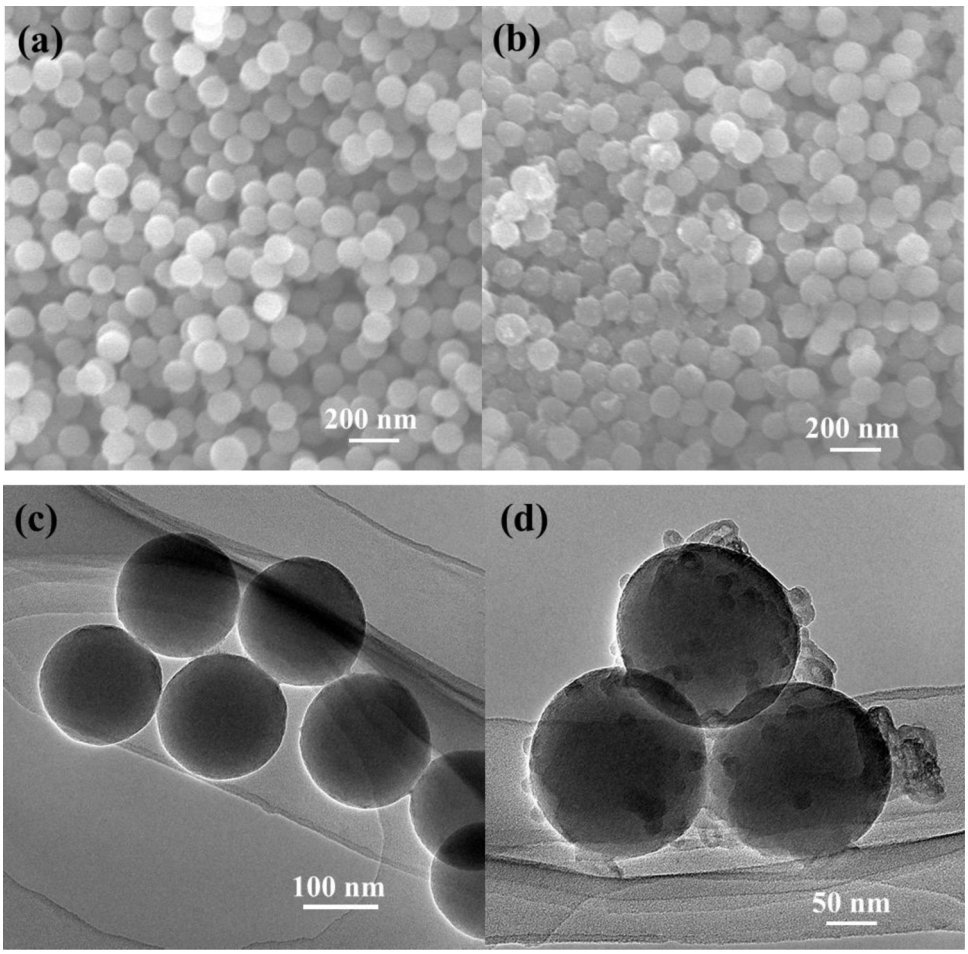

Fig. 1. The SEM and corresponding TEM images of (a, c) SiO_2 NPs and (b, d) SiO_2—Me&SO_3H NPs.

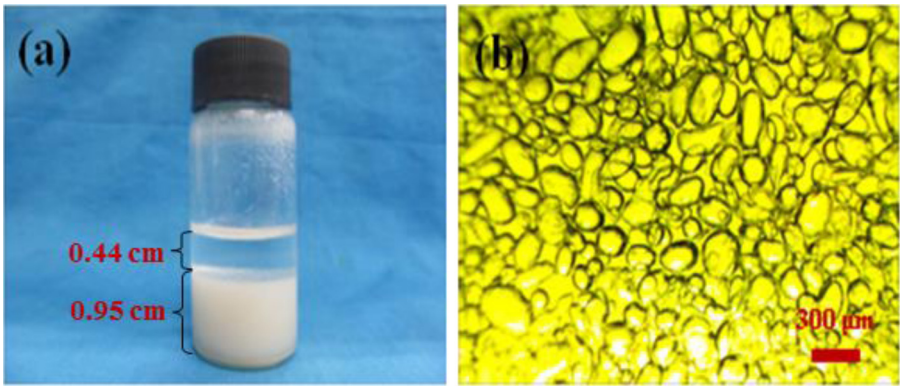

Fig. 2. (a) The digital photograph and (b) the corresponding optical microscopy image of SiO_2—Me&SO_3H NPs-stabilized Pickering emulsions.

that the functional groups were successfully grafted on the surface of the SiO_2—Me&SO_3H NPs. TGA was performed to analyze the grafting amount of organosilanes on the SiO_2—Me&SO_3H sample, and the results were shown in Fig. 3b. It can be seen that the SiO_2 NPs exhibited two main weight losses. The first rapid weight loss (~2.0 wt%) could be attributed to the removal of physisorbed water molecules on the sample surface when temperature was up to 150 °C. The second weight loss (~6.15 wt%) was due to decomposition of the oxygen-containing functional groups from SiO_2 NPs between 150 and 650 °C. In comparison, the weight losses of SiO_2—Me&SO_3H NPs were 1.6 wt% below 150 °C and 8.75% at temperature range of 150–800 °C, respectively. This clearly indicated that much more functional groups from SiO_2—Me&SO_3H NPs were decomposed at the second weight loss period than SiO_2 NPs. This remarkable weight loss could be attributed to the existence of —Me&SO_3H functional groups on the SiO_2—Me&SO_3H NPs because the organosulfonic acid required a higher decomposition temperature to achieve constant weight status.

To further determine the surface chemical composition of the SiO_2 NPs and SiO_2—CH_3&SO_3H catalyst, X-ray photoelectron spectroscopy (XPS) measurement was also carried out. As shown in Fig. 4, the XPS spectrum of the SiO_2—CH_3&SO_3H catalyst indicated that the specimen consisted of Si, O, C and S atoms as compared with pure SiO_2 NPs, whereas there was no S emission could be

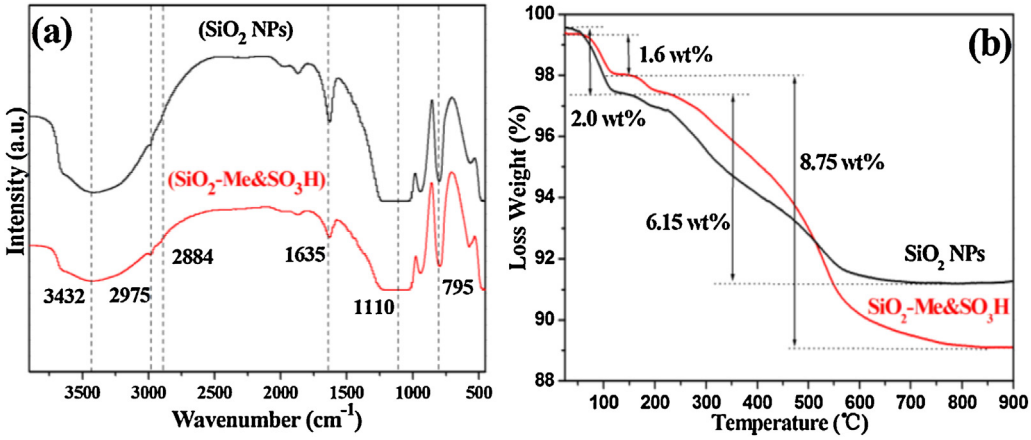

Fig. 3. (a) The FTIR spectra and (b) the TGA curves of SiO_2 NPs and SiO_2—Me&SO_3H NPs.

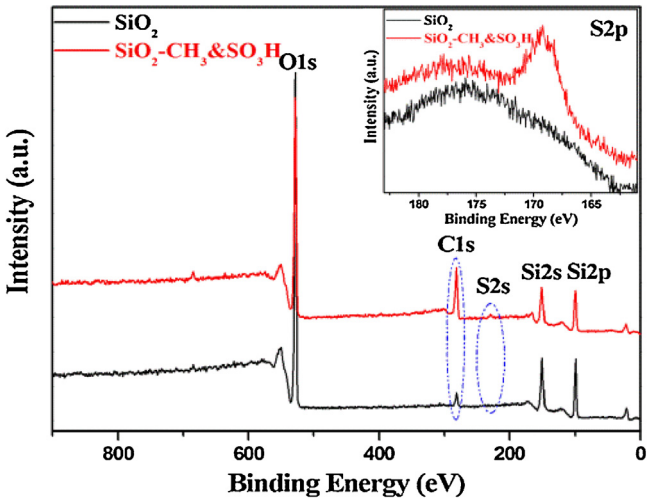

Fig. 4. The XPS spectra of SiO_2 NPs and SiO_2—CH_3&SO_3H catalyst (the insert image is the corresponding S2p curves).

detected in the spectrum and the signal of C_{1s} also had a remarkable increase from SiO_2—CH_3&SO_3H. In the inset image, the high resolution XPS spectrum showed a peak at 169 eV from SiO_2—CH_3&SO_3H sample which is assigned to S 2p from —SO_3H group [37]. As a result, XPS data further confirmed that the —CH_3 and —SO_3H groups were well-decorated on SiO_2 surface.

The deacetalization of aromatic and aliphatic acetal derivatives was chosen as the model reaction for the investigation of the catalytic performance of different catalysts (Table 1). The deacetalization of acetals to produce aldehyde derivatives represents an important pretreatment step in the production of pharmaceutical intermediates and fine chemicals based on aldehyde derivatives. Herein, four types of catalysts were initially carried out to illustrate the influence factors on the benzaldehyde dimethyl acetal, of which the toluene/water biphasic system was used as reaction solvent. When taking SiO_2 NPs and SiO_2—Me NPs as the catalyst, the benzaldehyde conversion was only 4.5% and 6.4% within 45 min, showing extremely low catalytic activity. We attributed the low catalytic activity to the lack of catalytic active sites. In contrast, the conversion reached up to 64.5% in the presence of SiO_2—SO_3H NPs, thus indicating that the sulfonic acid groups played a critical role in the deacetalization of acetal. Encouragingly, the benzaldehyde conversion reached up to 97% with the assistance of SiO_2—Me&SO_3H catalyst. (Table 1, entry 4). We reasoned that the excellent catalytic performance of SiO_2—Me&SO_3H catalyst was mainly attributed to the synergistic effect of the —SO_3H groups and —CH_3 groups. The —SO_3H groups behaved as the catalytic centers to release hydrogen ions, while the hydrophobic —CH_3 groups could greatly enrich the substrates around the catalytic active sites owing to the formation of Pickering emulsion.

To explore the generality of SiO_2—Me&SO_3H catalyst for deacetalization reaction, we examined conversion efficiency of a series of different substrates. As shown in Table 1, 4-methoxy benzaldehyde dimethyl acetal was transferred to 4-methoxy benzaldehyde and showed excellent conversion above 99% within 60 min. 1,1-dimethoxycyclohexane converted into cyclohexanone with 92.2% conversion within 60 min. 4-bromo-benzaldehyde dimethyl acetal deacetalized to 4-bromo-benzaldehyde at the conversion of 86.4%. Butanal dimethyl acetal was transferred to butanal with the conversion of 86.9% within 75 min. Moreover, the conversion of 4-methyl-2-phenyl-1,3-dioxolane was also reached up to 91.3% at 60 °C for 90 min. The possible reaction mechanism was presented in Fig. 5. Therefore, the SiO_2—Me&SO_3H catalyst has excellent catalytic ability for the deacetalization reaction.

In an attempt to investigate the solvent effect on the catalyst activity, we conducted the deacetalization of benzaldehyde dimethyl acetal in different solvent. As shown in Fig. 6a, the conversion of benzaldehyde dimethyl acetal was only 48.7% within 90 min in the toluene system, while in the toluene-water biphasic system it reached up to 92.7% within 45 min. It suggested that the toluene-water biphasic system was a better solvent for the reaction. Fig. 6b revealed that the SiO_2—Me&SO_3H catalyst displayed the higher catalytic activity when compared to SiO_2—SO_3H catalyst, and the SiO_2 NPs almost without any activity for the deacetalization. We next examined the influence of SiO_2—Me&SO_3H catalyst amount on the deacetalization reaction (Fig. 6c). Three parallel experimental groups with catalyst amount of 30, 45 and 60 mg were tested, respectively. It could be found that the highest reaction conversion occurred when catalyst amount was 45 mg. That was probably because the over-dosage (60 mg) led to the quenching of active centers of catalyst while the low-dosage (30 mg) could not provide sufficient active centers.

Last but not least, the recyclability of SiO_2—Me&SO_3H catalyst was examined in the deacetalization reaction of 4-bromobenzaldehyde dimethyl acetal under the described reaction conditions. Upon completion of each reaction, the reaction mixture was centrifuged and the upper toluene phase was withdrawn from the system by a syringe, and then a fresh of reactant and toluene was added into the above-mentioned catalyst aqueous solution for the subsequent reaction under the same reaction conditions. As can be seen in Fig. 7, no obvious change in the activity of the catalyst

Table 1
The deacetalization of acetal derivatives by SiO_2—Me&SO_3H catalyst.[a]

Entry	Catalyst	Substrate	Product	T (°C)	t (min)	Conv. (%)[b]
1	SiO_2	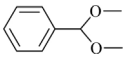	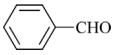	30	45	4.5
2	SiO_2—Me	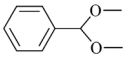	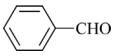	30	45	6.4
3	SiO_2—SO_3H	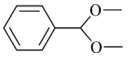	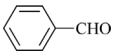	30	45	64.5
4	SiO_2—Me&SO_3H	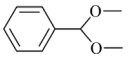	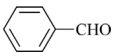	30	60	97.0
5	SiO_2—Me&SO_3H	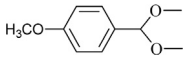	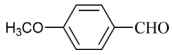	30	60	>99
6	SiO_2—Me&SO_3H	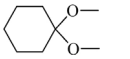	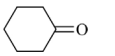	30	60	92.2
7	SiO_2—Me&SO_3H	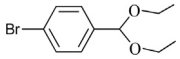	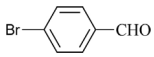	30	60	86.4
8	SiO_2—Me&SO_3H	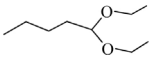		50	75	86.9
9	SiO_2—Me&SO_3H	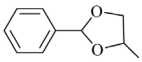	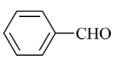	60	90	91.3

[a] Reaction conditions: 1.0 mmol substrate, 45 mg catalyst (6.3 μmol, S/C = 160), 3.0 mL toluene and 3.0 mL H_2O.
[b] The conversion was determined by GC (average conversion for three times), and the selectivity of the corresponding aldehydes >99%.

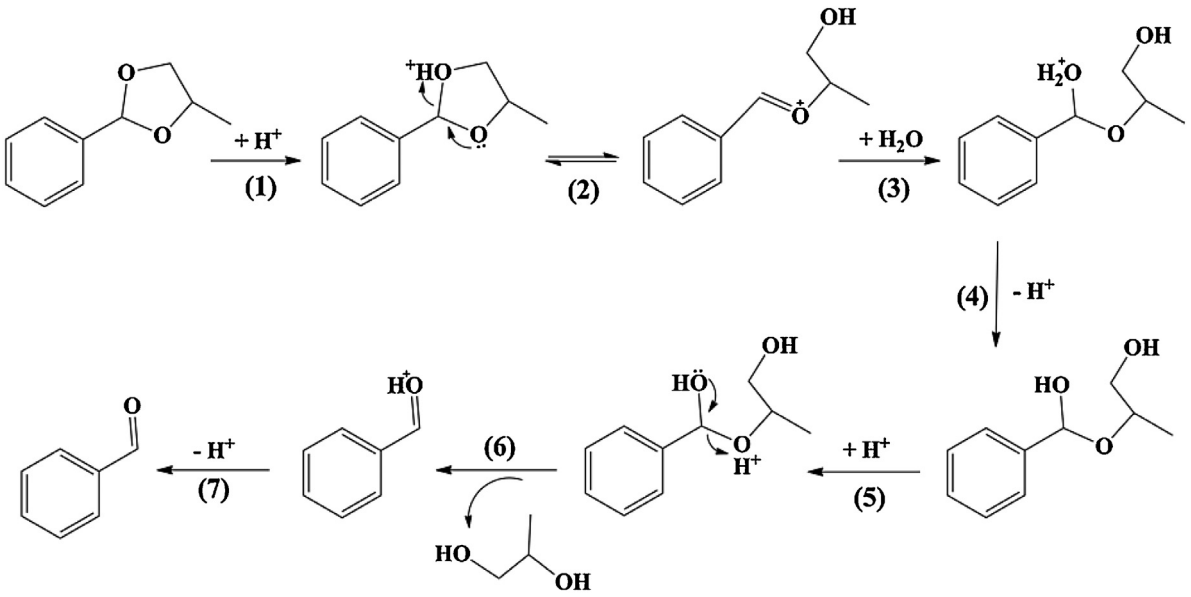

Fig. 5. The possible deacetalization mechanism of 4-methyl-2-phenyl-1,3-dioxolane.

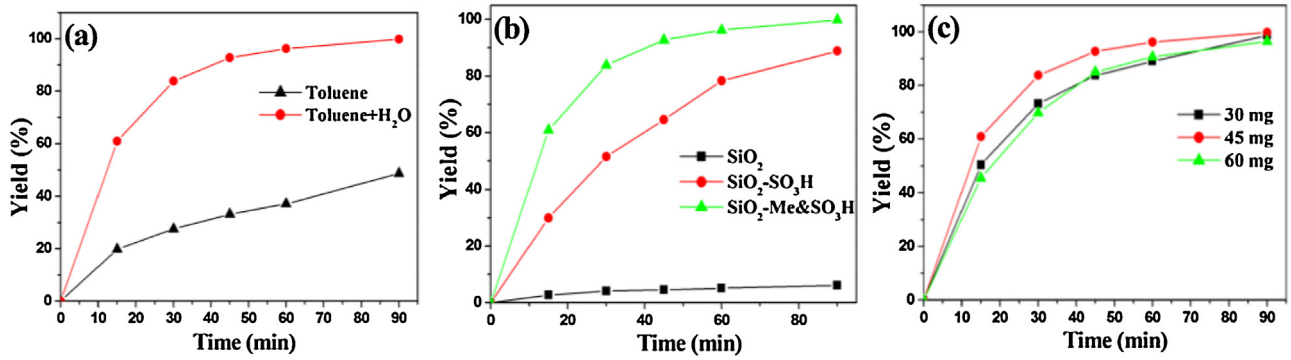

Fig. 6. The yield of benzaldehyde in the presence of (a) single and biphasic system, (b) different types of catalysts and (c) different amount of SiO_2—Me&SO_3H catalyst. Reaction conditions: 1.0 mmol of benzaldehyde dimethyl acetal, 3.0 mL of toluene and 3.0 mL H_2O.

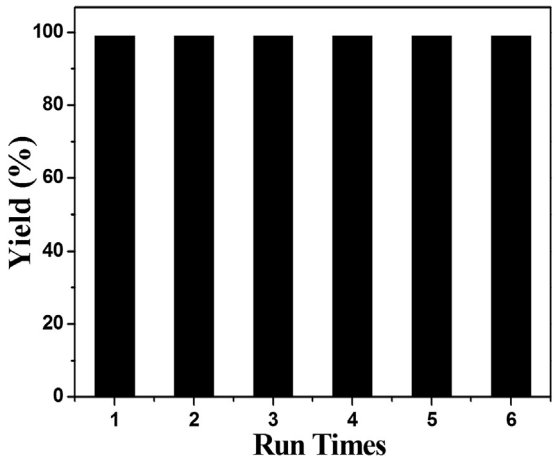

Fig. 7. The recyclability of the SiO_2—Me&SO_3H catalyst in deacetalization reaction.

was observed for at least 6 consecutive runs, suggesting the high stability in the deacetalization reaction.

4. Conclusion

In summary, a novel bifunctional SiO_2—Me&SO_3H catalyst containing both the hydrophobic methyl and hydrophilic sulfonic acid groups has been fabricated by mild surface modification of the silica nanoparticles. The as-prepared amphiphilic SiO_2—Me&SO_3H catalyst showed a high emulsifying performance, and a stabilized W/O Pickering emulsion could be generated. The obtained emulsion exhibited a high long-term stability and no water layer was separated from the emulsion within a period of more than one week. The SiO_2—Me&SO_3H stabilized emulsion presented an excellent catalytic activity for the deacetalization of aromatic and aliphatic acetal derivatives in a short period of time. The reasons can be attributed to the large interfacial area and low mass transfer resistance of countless micro-scale reactors. Our findings suggested that Pickering interfacial catalytic systems could be further widened by introducing other supports and active species.

Conflict of interest

The authors declare no competing financial interest.

Acknowledgements

This work was supported by the Scientific Research Start-up Funds of Shanxi University (023151801002) and Natural Science Foundation for Young Scientists of Shanxi Province (2015021051).

References

[1] W. Ramsden, Proc. R. Soc. London 72 (1903) 156–164.
[2] S.U. Pickering, J. Chem. Soc. 91 (1907) 2001–2021.
[3] F. Yang, S. Liu, J. Xu, Q. Lan, F. Wei, D. Sun, J. Colloid Interf. Sci. 302 (2006) 159–169.
[4] S. Frijters, F. Günther, J. Harting, Phys. Rev. E 90 (2014) 1–8.
[5] C. Huo, M. Li, X. Huang, H. Yang, S. Mann, Langmuir 30 (2014) 15047–15052.
[6] P.A. Kralchevsky, I.B. Ivanov, K.P. Ananthapadmanabhan, A. Lips, Langmuir 21 (2005) 50–63.
[7] S. Stiller, H. Gers-Barlag, M. Lergenmueller, F. Pflucker, J. Schulz, K.P. Wittern, R. Daniels, Colloids Surf. A 232 (2004) 261–267.
[8] S. Kango, S. Kalia, A. Celli, J. Njuguna, Y. Habibi, R. Kumar, Prog. Polym Sci. 38 (2013) 1232–1261.
[9] H. Liu, C. Wang, Q. Gao, X. Liu, Z. Tong, Acta Biomater. 6 (2010) 275–281.
[10] O. Kylian, A. Choukourov, H. Biederman, Thin Solid Films 548 (2013) 1–17.
[11] S. Crossley, J. Faria, M. Shen, D.E. Resasco, Science 327 (2010) 68–72.
[12] J. Peng, Q. Liu, Z. Xu, J. Masliyah, Energy Fuels 26 (2012) 2705–2710.
[13] A.D. Purceno, B.F. Machado, A.P.C. Teixeira, T.V. Medeiros, A. Benyounes, J. Beausoleil, H.C. Menezes, Z.L. Cardeal, R.M. Laqo, P. Serp, Nanoscale 7 (2015) 294–300.
[14] W. Zhang, L. Fu, H. Yang, ChemSusChem 7 (2014) 391–396.
[15] X.-R. Wei, J. Liu, Y. Yang, L. Deng, RSC Adv. 4 (2014) 35744–35749.
[16] H. Tan, P. Zhang, L. Wang, D. Yang, K. Zhou, Chem. Commun. 47 (2011) 11903–11905.
[17] X. Yang, Y. Liang, Y. Cheng, W. Song, X. Wang, Z. Wang, J. Qiu, Catal. Commun. 47 (2014) 28–31.
[18] X. Yang, Y. Liang, X. Zhao, Y. Song, L. Hu, X. Wang, Z. Wang, J. Qiu, RSC Adv. 4 (2014) 31932–31936.
[19] Z. Zhu, H. Tan, J. Wang, S. Yu, K. Zhou, Green Chem. 16 (2014) 2636–2643.
[20] P.A. Zapata, J. Faria, M.P. Ruiz, R.E. Jentoft, D.E. Resasco, J. Am. Chem. Soc. 134 (2012) 8570–8578.
[21] D.E. Resasco, Chin. J. Catal. 35 (2014) 798–806.
[22] M. Pera-Titus, L. Leclercq, J.-M. Clacens, F.D. Campo, V. Nardello-Rataj, Angew. Chem. Int. Ed. 54 (2015) 2006–2021.
[23] B.P. Binks, S.O. Lumsdon, Langmuir 16 (2000) 2539–2547.
[24] J. Zhou, X. Qiao, B.P. Binks, K. Sun, M. Bai, Y. Li, Liu, Langmuir 27 (2011) 3308–3316.
[25] X.M. Yang, X.N. Wang, C.H. Liang, W.G. Su, C. Wang, Z.C. Feng, C. Li, J.S. Qiu, Catal. Commun. 9 (2008) 2278–2281.
[26] L. Li, J. Lv, Y. Shen, X. Guo, L. Peng, Z. Xie, W. Ding, ACS Catal. 4 (2014) 2746–2752.
[27] I.F. Teixeira, A.A.S. Oliveira, T. Christofani, F.C.C. Moura, J. Mater. Chem. A 1 (2013) 10203–10208.
[28] M. Shen, D.E. Resasco, Langmuir 25 (2009) 10843–10851.
[29] J. Faria, M.P. Ruiz, D.E. Resasco, Adv. Synth. Catal. 352 (2010) 2359–2364.
[30] S. Ma, Y. Wang, K. Jiang, X. Han, Nano Res. 8 (2015) 2603–2610.
[31] C. Yu, L. Fan, J. Yang, Y. Shan, J. Qiu, Chem. Eur. J. 19 (2013) 16192–16195.
[32] S.P. Teong, G. Yi, H. Zeng, Y. Zhang, Green Chem. 17 (2015) 3751–3755.
[33] Y. Qu, R. Huang, W. Qi, R. Su, Z. He, ACS Appl. Mater. Interfaces 7 (2015) 14954–14964.
[34] W.-J. Zhou, L. Fang, Z. Fan, B. Albela, L. Bonneviot, F.D. Campo, M. Pera-Titus, J.-M. Clacens, J. Am. Chem. Soc. 136 (2014) 4869–4872.
[35] F. Zhang, H. Yang, Catal. Sci. Technol. 5 (2015) 572–577.
[36] A. Mobaraki, B. Movassagh, Karimi, Appl. Catal. A: Gen. 472 (2014) 123–133.
[37] J.F. Moudler, W.F. Stickle, P.E. Sobol, K.D. Bomben, Handbook of X-ray Photoelectron Spectroscopy, PerkinElmer, 1992, 2015.